Supporting Information

# 3D current collector based on cellulose-carbon nanotube nanocomposites for all-solid-state batteries

*Sejung Park*[#a], *Young-Woong Song*[#b,c], *Boeun Ryu*[a], *Hojin Son*[a], *Min-Young Kim*[c], *Jeakook Kim*[b], *Jinsub Lim*[c], *and Changhun Yun*[*a]

[a] School of Polymer Science and Engineering, Chonnam National University, Gwangju 61186, Republic of Korea

[b] Department of Materials Science and Engineering, Chonnam National University, Gwangju 61186, Republic of Korea

[c] Korea Institute of Industrial Technology (KITECH), Gwangju 61012, Republic of Korea

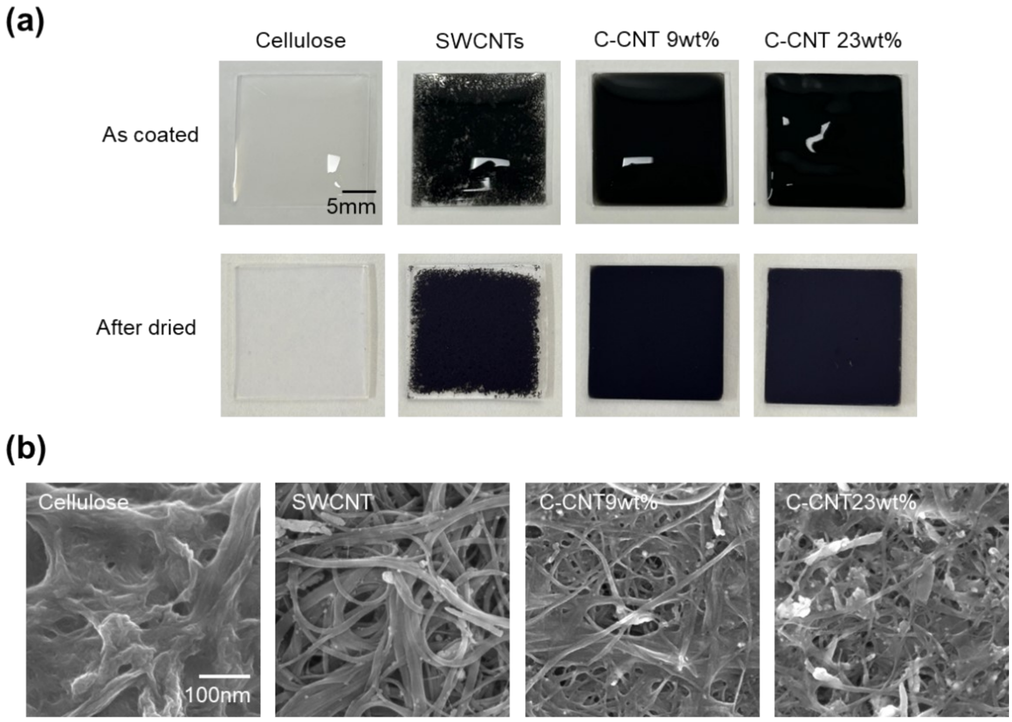


**Figure S1.** (a) Photographs of drop-cast samples before and after the drying process. The aqueous dispersion of pulp cellulose or only single walled carbon nanotubes (SWCNTs) were prepared after shaking for 240 min. The highly conductive inks based on cellulose-SWCNTs (C-CNTs) consisting of 9 wt% and 23 wt% SWCNTs were obtained with the shaking time of 40 minutes and 160 minutes, respectively. (b) High-resolution SEM images at the surface of the prepared drop-cast samples.

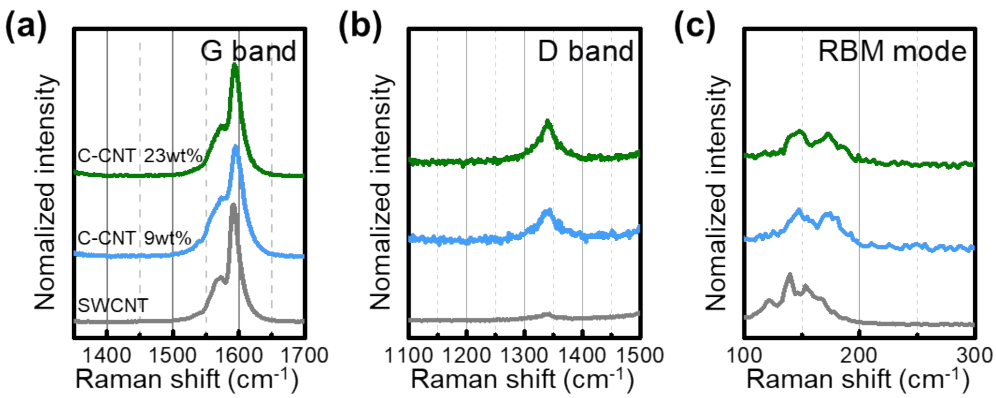


**Figure S2.** The enlarged Raman spectra of the tested sample in Figure 1f at G-band peaks, D-band peaks, and radial-breathing-mode (RBM) peaks.

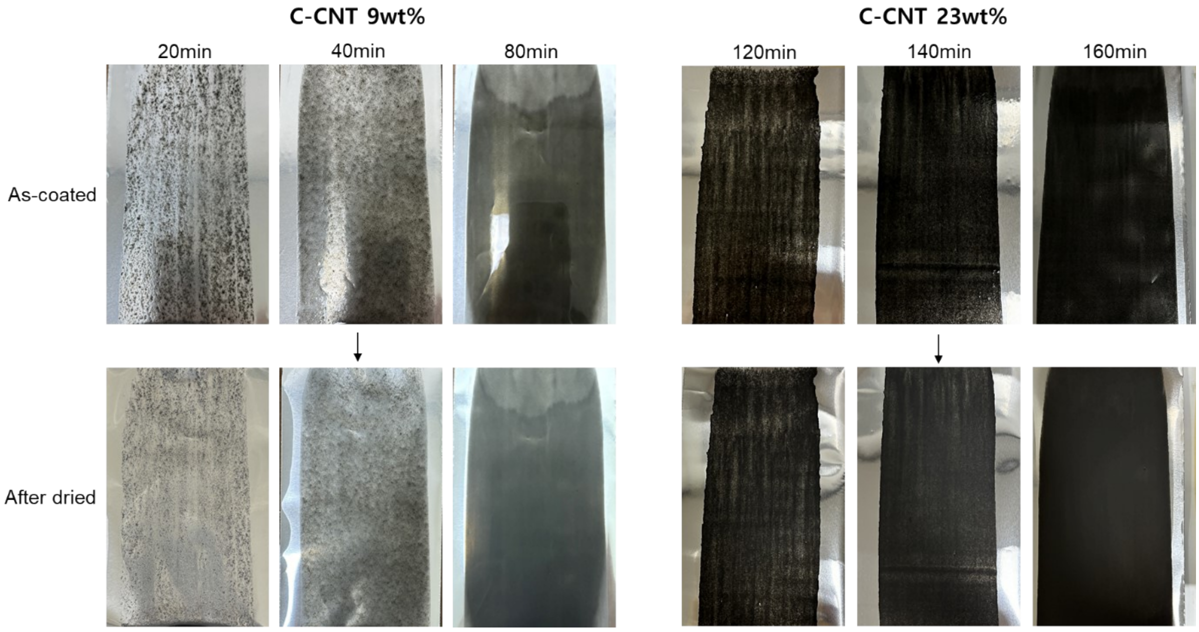


**Figure S3.** Photograph of (Top) the as-coated C-CNT inks on an Al foil using a manual bar coater and (bottom) the dried C-CNT films on an Al foil. The conductive C-CNT inks consisting of 9 wt % and 23 wt% SWCNTs were prepared as increasing the target shaking time from 20 minutes to 160 minutes.

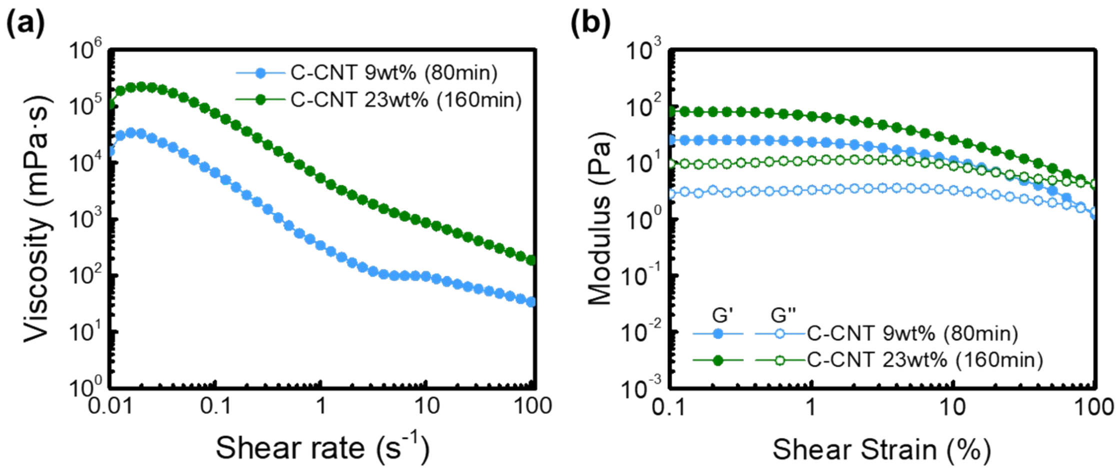


**Figure S4.** Rheological properties of the tested conductive C-CNT inks consisting of 9 wt% and 23 wt% SWCNTs. (a) Steady shear viscosity from the rotational shear modes (b) Amplitude sweep test from the oscillatory shear modes (solid symbols are G' and open symbols are G"),

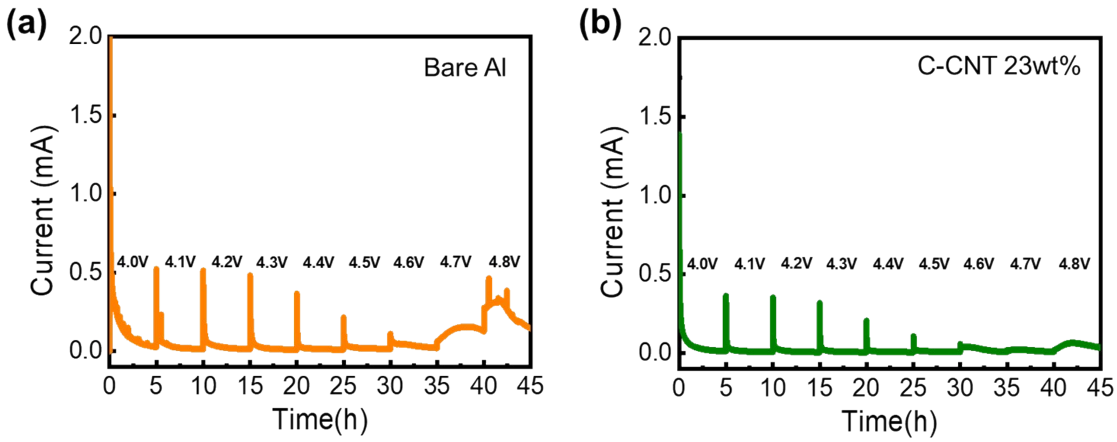


**Figure S5.** The electrochemical floating test for the tested ASSBs using (a) aluminum current collector and (b) the hybrid current collector with 23 wt% C-CNT.

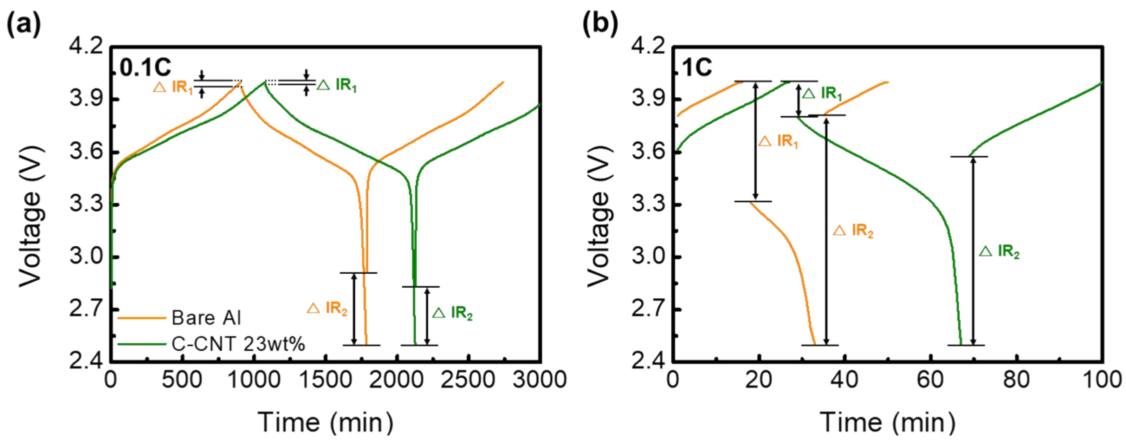


**Figure S6.** Galvanostatic charge/discharge of the tested ASSBs using Al current collector and the hybrid current collector (consisting of 23 wt% C-CNT coating on Al foil) at charge/discharge rates of (a) 0.1 C and (b) 1.0 C. IR-drop data is obtained when charging is switched to discharging ($\Delta IR_1$) and when discharging is switched to charging ($\Delta IR_2$).

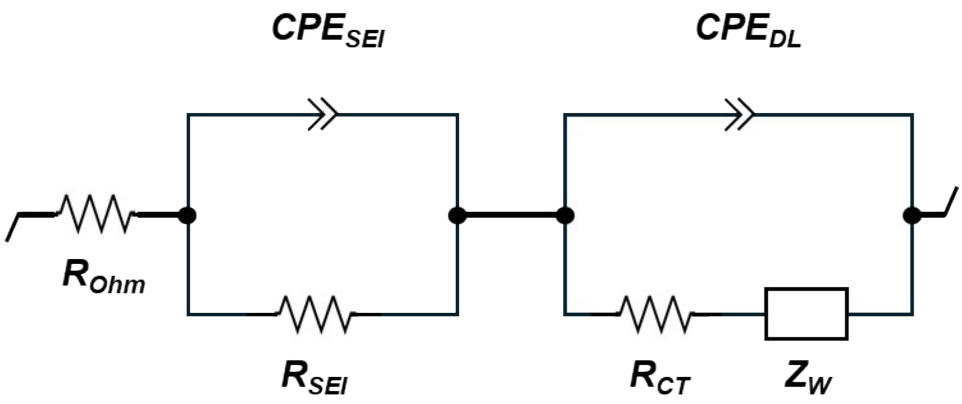


**Figure S7.** Equivalent circuit used for fitting the measured impedance data. $CPE_{SEI}$ and $CPE_{DL}$ are constant phase elements corresponding to the solid interface interlayer (SEI) and the double-layer formation during charging/discharging. $R_{Ohm}$, $R_{SEI}$, $R_{CT}$, and $Z_W$ represent the ohmic resistance, the SEI layer resistance, the charge-transfer resistance, and Warburg (diffusion) impedance from the Li-ion diffusion, respectively.

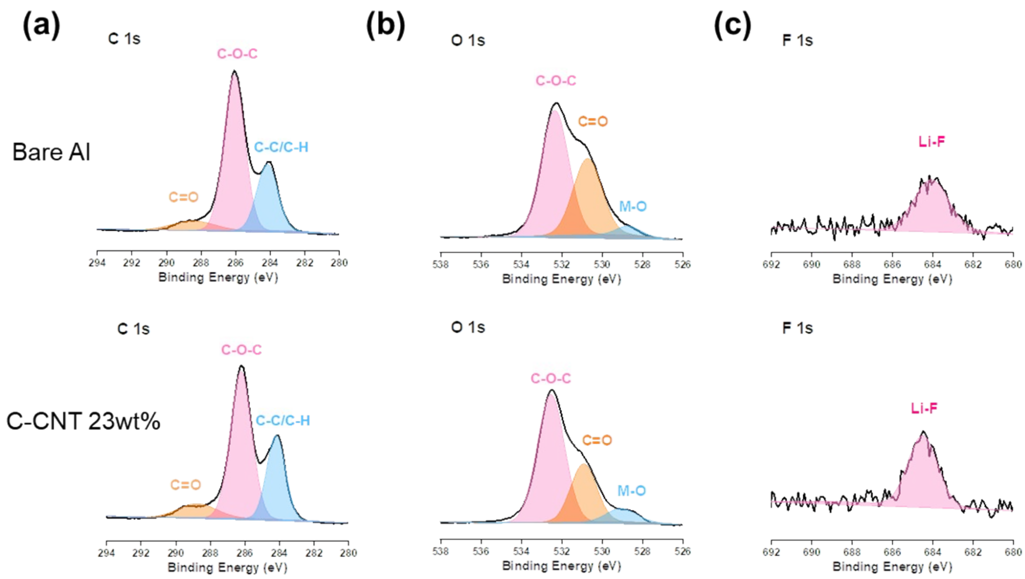


**Figure S8.** (a) C 1s, (b) O 1s, and (c) F 1s XPS spectra of the NCM-based cathode electrode using fully charged electrodes after 100 cycles. Top and bottom of XPS results correspond to ASSBs based on bare aluminum current collector and hybrid current collector with 23 wt% C-CNT, respectively.

**Table S1.** The electrical characteristics of C-CNT films with various shaking times.

| The drop-casted C-CNT film with 9 wt% SWCNTs | | | | | | |
|---|---|---|---|---|---|---|
| $t_{Shake}$ | 40 min | 80 min | 120 min | 160 min | 200 min | 240 min |
| **Sheet resistance ($\Omega$ sq$^{-1}$)** | 15.5 (±1.2) | 43.7 (±0.1) | 84.9 (±0.2) | 599.0 (±0.4) | 883.0 (±8.7) | 1390.0 (±2.8) |
| **Thickness (μm)** | 6.3 (±0.2) | 6.7 (±0.15) | – | – | – | – |
| **Conductivity (S cm$^{-1}$)** | 102.4 | 34.2 | – | – | – | – |
| **The drop-casted C-CNT film with 23 wt% SWCNTs** | | | | | | |
| $t_{Shake}$ | 40 min | 80 min | 120 min | 160 min | 200 min | 240 min |
| **Sheet resistance ($\Omega$ sq$^{-1}$)** | 21.7 (±3.6E-02) | 8.6 (±1.4E-02) | 7.6 (±1.5E-02) | 6.6 (±4.4E-16) | 10.3 (±1.1E-02) | 34.1 (±4.4) |
| **Thickness (μm)** | 8.2 (±0.17) | – | – | 8.4 (±0.2) | – | 8.7 (±0.3) |
| **Conductivity (S cm$^{-1}$)** | 56.1 | – | – | 180.3 | – | 33.7 |

**Table S2.** The calculated IR drops in the tested ASSBs with various current collectors at different C-rates of 0.1 C and 1.0 C. IR drops were obtained from the Galvanostatic charge/discharge curves in Figure S5.

| | **Bare Al** | | **C-CNT 23 wt%** | |
|---|---|---|---|---|
| **Current density (C-rate)** | 0.1 C | 1.0 C | 0.1 C | 1.0 C |
| **$\Delta IR_1$ (V)** | 0.03048 | 0.68955 | 0.01742 | 0.20214 |
| **$\Delta IR_2$ (V)** | 0.41816 | 1.31108 | 0.33742 | 1.07707 |
| **$\Delta IR_{Total}$ (V)** | 0.44864 | 2.00063 | 0.35484 | 1.27921 |

**Table S3.** The extracted results of $R_{Ohm}$, $R_{SEI}$, and $R_{CT}$ from the Nyquist plot in Figure 4c using the equivalent circuit depicted in Figure S6. Warburg coefficient and the corresponding Li-ion diffusion coefficient were calculated using the measured EIS result in the low-frequency region (0.15–2.3 Hz).

| | **1$^{st}$ Bare Al** | **1$^{st}$ C-CNT 23 wt%** | **100$^{th}$ Bare Al** | **100$^{th}$ C-CNT 23 wt%** |
|---|---|---|---|---|
| **$R_{Ohm}$ (Ω)** | 24.8 | 25.7 | 39.2 | 25.0 |
| **$R_{SEI}$ (Ω)** | 50.4 | 12.6 | 119.5 | 19.4 |
| **$R_{CT}$ (Ω)** | 119.1 | 10.6 | 252.9 | 10.8 |
| **Warburg coefficient ($\sigma$, Ω $s^{-1/2}$)** | 34.2 | 29.1 | 58.7 | 51.5 |
| **Li-ion diffusion coefficient ($D_{Li+}$, $cm^2$ $s^{-1}$)** | $4.74 \times 10^{-16}$ | $6.55 \times 10^{-16}$ | $1.61 \times 10^{-16}$ | $2.10 \times 10^{-16}$ |